Bolometric effect in a waveguide-integrated graphene photodetector*

Yubing Wang(王玉冰), Weihong Yin(尹伟红), Qin Han(韩勤)†, Xiaohong Yang(杨晓红), Han Ye(叶焓), Qianqian Lv(吕倩倩), and Dongdong Yin(尹冬冬)

State Key Laboratory on Integrated Optoelectronics, Institute of Semiconductors, Chinese Academy of Sciences, Beijing 100083, *China*

(Received 20 June 2016; revised manuscript received 13 July 2016; published online 30 September 2016)

Graphene is an alternative material for photodetectors owing to its unique properties. These include its uniform absorption of light from ultraviolet to infrared and its ultrahigh mobility for both electrons and holes. Unfortunately, due to the low absorption of light, the photoresponsivity of graphene-based photodetectors is usually low, only a few milliamps per watt. In this letter, we fabricate a waveguide-integrated graphene photodetector. A photoresponsivity exceeding 0.11 A·W^{-1} is obtained which enables most optoelectronic applications. The dominating mechanism of photoresponse is investigated and is attributed to the photo-induced bolometric effect. Theoretical calculation shows that the bolometric photoresponsivity is 4.6 A·W^{-1}. The absorption coefficient of the device is estimated to be 0.27 dB·μm^{-1}.

Keywords: graphene photodetector, graphene bolometer, bolometric effect, waveguide integration

PACS: 81.05.ue, 85.60.Dw **DOI:** 10.1088/1674-1056/25/11/118103

1. Introduction

Graphene, one layer of carbon atoms arranged in a hexagonal lattice, has received tremendous research interest since its first realization.[1] Graphene-based devices, such as transistors,[2–4] gas sensors[5] and optical modulators[6–8] exhibit a number of merits. Particularly, owing to its extremely high mobility for both electrons and holes[9] and its uniform light absorption coefficient (∼2.3%) over a wide range of spectrum from ultraviolet to infrared,[10,11] different kinds of graphene-based photodetectors have been designed and fabricated.[12–25] The field-effect-transistor-structure graphene photodetectors are the most common ones.[12–14] However, since the photo-generated electrons and holes can be separated only in the vicinity of the metal leads (∼ 200 nm), its photoresponsivity is rather low, only a few milliamps per watt.[12] To improve the interaction between graphene and light, microcavity integrated graphene photodetectors are realized and a responsivity of 21 mA·W^{-1} is obtained.[23,24] However, this type of graphene photodetector requires a rather complicated fabrication process such as epitaxial growth of Bragg mirror and buffer layers.[24] An alternative way to acquire high photoresponsivity is a waveguide-integrated graphene photodetector, which enhances the absorption efficiency and lengthens the absorption length along the waveguide.[25] Recently, Li *et al*. experimentally reported a maximum of absorption coefficient of 0.2 dB·μm^{-1} by locating graphene directly on the top of a waveguide.[26] In this letter, we fabricate a waveguideintegrated graphene photodetector using a wet transfer method to transfer an individual graphene microsheet to the specific position of a waveguide. A photoresponsivity exceeding 0.11 A·W^{-1} is obtained which enables most optoelectronic applications. There are several different processes that convert photons into an electrical signal in graphene. These involve the photovoltaic effect, the photothermoelectric effect, and the bolometric effect. The dominating mechanism of photoresponse is investigated and is attributed to the photo-induced bolometric effect. Theoretical calculation shows that the bolometric photoresponsivity is 4.6 A·W^{-1}. The absorption coefficient of the device is estimated to be 0.27 dB·μm^{-1}, which is consistent with Li's result.

2. Device fabrication

The device fabrication starts with a wet transfer process. Briefly, a graphene sample is mechanically exfoliated on a Si/SiO_2 substrate. Then a layer of poly (methyl methacrylate) (PMMA) is spin-coated on the Si/SiO_2 substrate. Then the PMMA membrane is released in 1 mol·L^{-1} NaOH solution at 80 °C. The released PMMA membrane is then thoroughly cleaned in deionized water and dried in N_2 flow. Then it is fixed to a home-made micrometer manipulator. Synchronously, a standard electron-beam lithography (EBL) is performed on the target substrate to pattern a transfer window for the graphene sample. Then the target substrate, with a drop of deionized water on its surface, is located on the wafer carrier of a microscope. Then the PMMA membrane and the target substrate are brought into contact. By adjusting the micrometer manipulator and the wafer carrier of the microscope, we can align the graphene sample to the target position. Once aligned, the whole set up is left in ambient condition

*Project supported by the National Key Research and Development Program of China (Grant No. 2016YFB0402204), the High-Tech Research and Development Program of China (Grant Nos. 2013AA031401, 2015AA016902, and 2015AA016904), and the National Natural Science Foundation of China (Grant Nos. 61674136, 61176053, 61274069, and 61435002).

†Corresponding author. E-mail: hanqin@semi.ac.cn

© 2016 Chinese Physical Society and IOP Publishing Ltd

for 12 hours. To further increase the interaction between the graphene sample and the substrate, the substrate is baked at 120 °C for 15 minutes. Then, it is cleaned in acetone, ethanol, and deionized water, leaving the graphene sample on the target position. The electrodes are fabricated by EBL followed by electron-beam evaporation (EBE) of 20 nm Ti and 70 nm Au. Finally, the device is thermally annealled in H_2 and Ar mixture flow at 400 °C for 2 hours.

3. Results and discussion

A false-color top-view scanning-electron-microscope (SEM) image of the device is shown in Fig. 1(a). The length and width of graphene channel are 3 μm and 60 μm, respectively. Figure 1(b) shows the zoom-in view of the region indicated by the dash box in Fig. 1(a). In the vicinity of the waveguide there is 300-nm-wide graphene suspending in air. Also, graphene crimples and locally bulges during the transfer process. Figure 1(c) shows the Raman spectrum of the device at 488 nm. The ratio of I_{2D}/I_G is 1.56, indicating graphene is single layer. The weak D peak around 1350 cm^{-1} may result from graphene crimps and bulges.

The light source is a DFB laser operating at 1550 nm, amplified by EDFA and calibrated by an optical power meter (10 mW). Light is coupled in and out of the waveguide through two gratings which are designed particularly for a wavelength of 1550 nm. The coupling coefficient of each grating is measured to be 14%, corresponding to an incident power of 1.4 mW in the waveguide. Figure 1(d) shows the cross-section view of the device structure and the optical field distribution in the waveguide. The optical field distribution is simulated by finite-difference time-domain (FDTD) solutions. The waveguide is designed to maximize the evanescent absorption of graphene. The metal leads are far enough (∼ 1.5 μm) so as to have negligible effects on the optical mode. All tests are performed in ambient conditions at room temperature.

Current I as a function of bias voltage V_b with and without illumination is plotted in Fig. 2(a). Unlike conventional grapheme photodetectors,[12,13] an apparent photo-induced reduction in current is obtained. We attribute this phenomenon to the graphene bolometric effect as discussed below. As shown in Fig. 2(b), a photocurrent as high as 0.16 mA is achieved at 1 V bias voltage, corresponding to a photoresponsivity of 0.11 $A{\cdot}W^{-1}$. There is no sign of saturation of photocurrent at 1 V bias, yet to avoid electrical breakdown V_b is limited within 1 V.

We now move on to discuss the photoresponse mechanism of the device. Generally, there are three effects that contribute to the photocurrent. The first is the photovoltaic effect (PVE) where light-excited electrons and holes are driven in opposite directions and are collected by electrodes within their lifetime, producing the photocurrent.[12–16] However, this is obviously not the dominant photocurrent mechanism of the device, since if so there should be an increase rather than a reduction of current when illuminated. Therefore the photovoltaic effect is negligible in our device.

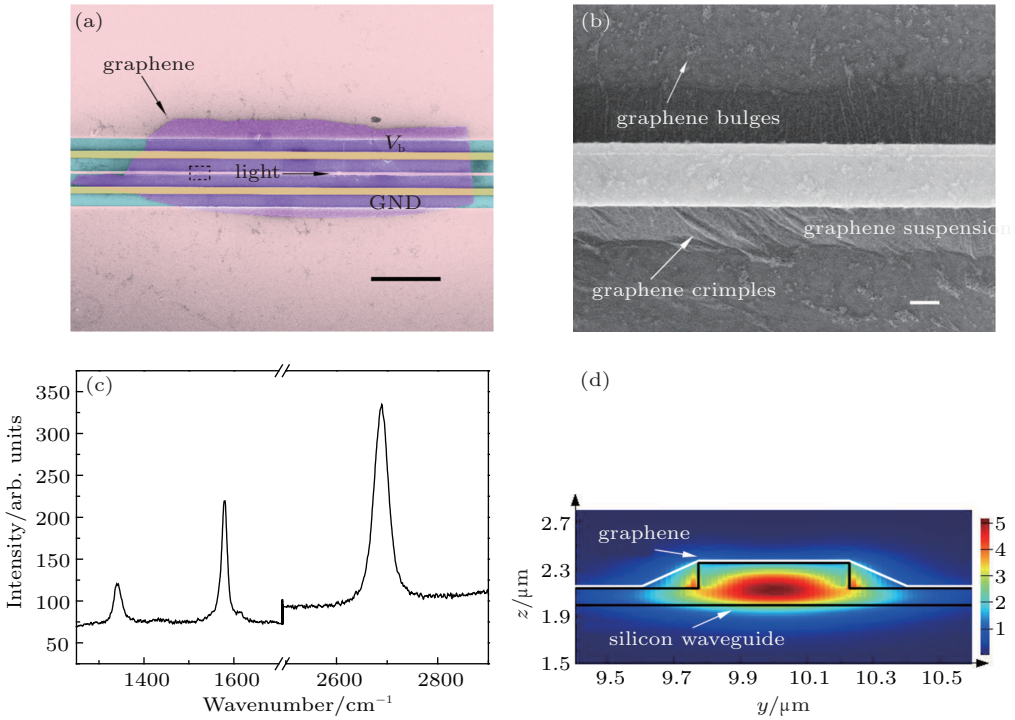


Fig. 1. (a) A false-color topview SEM image of the device, displaying graphene (purple), metal leads (yellow), unetched silicon (pink), and etched region (green). Scale bar, 10 μm. (b) A zoom-in view of the region indicated by dash box in Fig. 1(a), showing graphene crimples and bulges. Scale bar, 200 nm. (c) The Raman spectrum of the device at 488 nm. (d) The cross-section view of the device structure and the optical field distribution in waveguide.

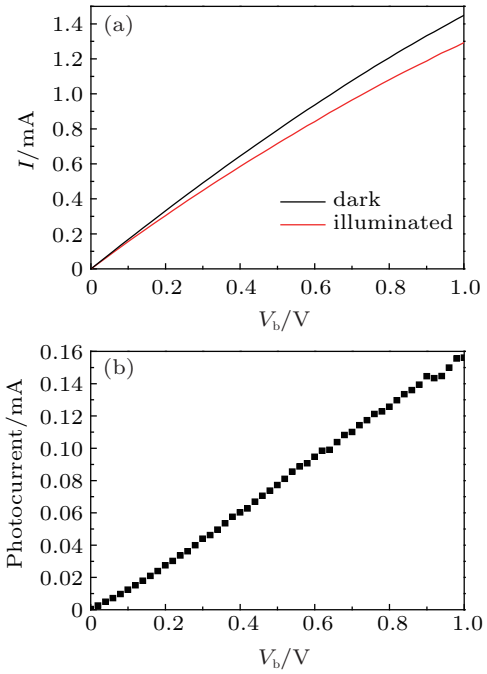


Fig. 2. (a) Current I as a function of bias voltage V_b with and without illumination. (b) The photocurrent versus V_b curve. V_b is limited within 1 V.

The second is the photo-thermoelectric effect (PTE), where according to the Seebeck effect, both temperature gradient and chemical potential gradient generate a thermoelectric current.[17–20] In the case of our device, light absorption generates the temperature gradient perpendicular to the waveguide and electrical bias breaks the balance of the chemical potential gradient although graphene is homogenously doped. The photocurrent generated by PTE is determined by

$$I_{\mathrm{PTE}} = \frac{(S_1 - S_2)\Delta T}{R}, \tag{1}$$

where S is the Seebeck coefficient of graphene, ΔT is the temperature gradient, and R is the resistance. The Seebeck coefficient S is determined by the Mott formula[19,27,28]

$$S = -\frac{\pi^2 k_{\mathrm{B}}^2 T}{3e}\frac{1}{\sigma}\frac{\mathrm{d}\sigma}{\mathrm{d}\varepsilon}, \tag{2}$$

where k_{B} is Boltzmann constant, T is temperature, e is elementary charge, σ is conductivity of graphene, and ε is electron energy. Assuming the heat flow as a radical wave, the temperature gradient is determined by[19]

$$\Delta T = \frac{P\alpha}{2\pi k d}, \tag{3}$$

where P is incident power, α is the absorption coefficient of graphene, $\kappa = 5000\ \mathrm{W{\cdot}m^{-1}{\cdot}K^{-1}}$ is the thermal conductivity of single layer graphene,[29] and $d = 0.34$ nm is the thickness of graphene. Therefore ΔT is calculated to be 2.9 K. Taking $(S_1 - S_2) = 100\ \mu\mathrm{V{\cdot}K^{-1}}$, which is reasonable,[17–19,27,28] I_{PTE} is calculated to be 0.35 μA, in opposite direction to experimentally measured photocurrent and three orders of magnitudes smaller than the measured valve. Therefore the photo-thermoelectric effect is not the dominant effect of the device.

The only possible explanation of our observation is the photo-bolometric effect (PBE), where light absorption elevates the local temperature of graphene by strong electron-phonon interaction, which in turn enhances the electron-acoustic phonon scattering, leading to an increase of resistance, i.e., a reduction of current.[21,30] Since PBE is resistance related, we thus

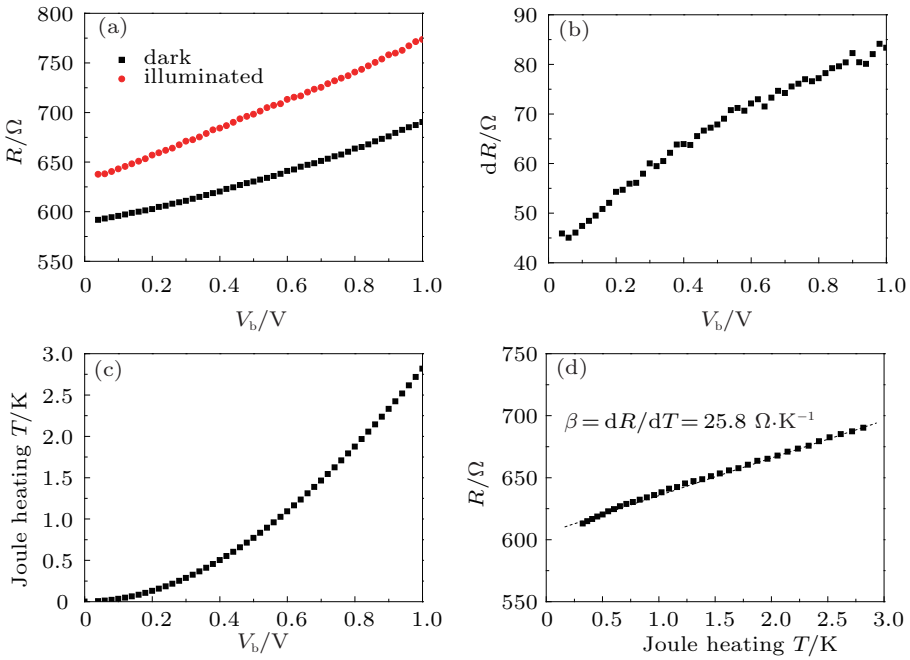


Fig. 3. (a) The R–V_b curve with and without illumination; (b) the resistance change induced by photo illumination as a function of bias voltage V_b; (c) the calculated Joule heating T as a function of bias voltage V_b; (d) the correlation between resistance R and Joule heating K. The bolometric effect coefficient β is extracted to be 25.8 $\Omega{\cdot}\mathrm{K}^{-1}$.

convert Fig. 2(a) into an R–V_b curve by Ohm law, as shown in Fig. 3(a). The photo-induced resistance change dR as a function of bias voltage V_b is shown in Fig. 3(b). When illuminated, the resistance change at 1 V is 83.3 Ω. It is well known that the presence of electrical power can heat up graphene through Joule heating,[21,22,31,32] which is measured to be 3.5 K per kW·cm^{-2}.[32] The calculated Joule heating T as a function of bias voltage V_b is plotted in Fig. 3(c). Then we have the correlation between Joule heating T and resistance R, as shown in Fig. 3(d). The bolometric effect coefficient β, defined as the change in resistance dR divided by the change in temperature dT, is extracted to be 25.8 Ω·K^{-1}, exhibiting a metallic transport characteristic. Then the change in temperature resulting from infrared radiation absorption dT is 3.2 K. According to Eq. (3), photo power absorbed by graphene is calculated to be 34.3 μW, corresponding to a bolometric photoresponsivity of 4.6 A·W^{-1}. Simple calculation shows the absorption coefficient of the device is 0.27 dB·μm^{-1}, consistent with Ref. [26].

4. Conclusion

In conclusion, we have fabricated a waveguide-integrated graphene photodetector using a wet transfer method to transfer an individual graphene microsheet to the specific position of a waveguide. A photoresponsivity exceeding 0.11 A·W^{-1} is obtained which enables most optoelectronic applications. The mechanism of the photoresponse is investigated and is attributed to the photo-induced bolometric effect. Theoretical calculation shows that the bolometric photoresponsivity is 4.6 A·W^{-1}. The absorption coefficient of the device is estimated to be 0.27 dB·μm^{-1}.

References

[1] Novoselov K S, Geim A K, Morozov S V, Jiang D, Zhang Y, Dubonos S V, Grigorieva I V and Firsov A A2004 *Science* **3** 669
[2] Wang X, Shi Y and Zhang R 2013 *Chin. Phys. B* **22** 098505
[3] Liao L, Lin Y C, Bao M Cheng R, Bai J, Liu Y, Qu Y, Wang K L, Huang Y and Duan X 2010 *Nature* **467** 305
[4] Wu H, Linghu C, Lv H and Qian H 2013 *Chin. Phys. B* **22** 098106
[5] Schedin F, Geim A K, Morozov S V Hill E W, Blake P, Katsnelson M I and Novoselov K S 2007 *Nat. Mater.* **6** 652
[6] Liu M, Yin X, Ulin-Avila E, Geng B, Zentgraf T, Ju L, Wang F and Zhang X 2011 *Nature* **474** 64
[7] Li W, Chen B, Meng C Fang W, Xiao Y, Li X, Hu Z, Xu Y, Tong L, Wang H, Liu W, Bao J and Shen Y R 2014 *Nano Lett.* **14** 955
[8] Liu M, Yin X and Zhang X 2012 *Nano Lett.* **12** 1482
[9] Bolotin K I, Sikes K J, Jiang Z Klima M, Fudenberg G, Hone J, Kim P and Stormer H L 2008 *Solid State Commun.* **146** 351
[10] Yin W, Han Q and Yang X 2012 *Acta Phys. Sin.* **61** 248502 (in Chinese)
[11] Nair R R, Blake P, Grigorenko A N Novoselov K S, Booth T J, Stauber T, Peres N M R and Geim A K 2008 *Science* **320** 1308
[12] Mueller T, Xia F and Avouris P 2010 *Nat. Photonics* **4** 297
[13] Yin W, Wang Y, Han Q and Yang X 2015 Chin. Phys. B 24 068101
[14] Lee E J H, Balasubramanian K,Weitz R T Burghard M and Kern K 2008 *Nat. Nanotechnol.* **3** 486
[15] Peters E C, Lee E J H, Burghard M and Kern K 2010 *Appl. Phys. Lett.* **97** 193102
[16] Xia F, Mueller T, Golizadeh-Mojarad R Freitag M, LinY M, Tsang J, Perebeinos V and Avouris P 2009 *Nano Lett.* **9** 1039
[17] Lemme M C Koppens F H L, Falk A L Rudner M S, Park H, Levitov L S and Marcus C M 2011 *Nano Lett.* **11** 4134
[18] Gabor N M Song J C W, Ma Q Nair N L, Taychatanapat T, Watanabe K, Taniguchi T, Levitov L S and Jarillo-Herrero P 2011 *Science* **334** 648
[19] Xu X, Gabor N M, Alden J S van der Zande A M and McEuen P L 2010 *Nano Lett.* **10** 562
[20] Sun D, Aivazian G, Jones A M Ross J S, Yao W, Cobden D and Xu X 2012 *Nat. Nanotechnol.* **7** 114
[21] Freitag M, Low T, Xia F and Avouris P 2013 *Nat. Photonics* **7** 53
[22] Mahjoub A M, Suzuki S, Ouchi T, Aoki N, Miyamoto K, Yamaguchi T, Omatsu T, Ishibashi K and Ochiai Y 2015 *Appl. Phys. Lett.* **107** 083506
[23] Engel M, Steiner M, Lombardo A Ferrari A C, Lohneysen H v Avouris P and Krupke R 2012 *Nat Commun* **3** 906
[24] Furchi M, Urich A, Pospischil A Lilley G, Unterrainer K, Detz H, Klang P, Andrews A M, Schrenk W, Strasser G and Mueller T 2012 *Nano Lett.* **12** 2773
[25] Schall D, Neumaier D Mohsin M Chmielak B, Bolten J, Porschatis C, Prinzen A, Matheisen C, Kuebart W, Junginger B, Templ W, Giesecke A L and Kurz H 2014 *ACS Photonics* **1** 781
[26] Li H, Anugrah Y, Koester S J and Li M 2012 *Appl. Phys. Lett.* **101** 111110
[27] Wei P, Bao W, Pu Y Lau C N and Shi J 2009 *Phys. Rev. Lett.* **102** 166808
[28] Zuev Y M, Chang W and Kim P 2009 *Phys. Rev. Lett.* **102** 096807
[29] Balandin A A, Ghosh S, Bao W Calizo I, Teweldebrhan D, Miao F and Lau C N 2008 *Nano Lett.* **8** 902
[30] Chen J H, Jang C, Xiao S Ishigami M and Fuhrer M S 2008 *Nat Nanotechnol.* **3** 206
[31] Moser J, Barreiro A and Bachtold A 2007 *Appl. Phys. Lett.* **91** 163513
[32] Freitag M, Steiner M, Martin Y, Perebeinos V, Chen Z, Tsang J C and Avouris P 2009 *Nano Lett.* **9** 1883